2025 *Egypt. J. Chem.* **Vol. 67**, No. 7 pp. 263 - 274 (2024)

Egyptian Journal of Chemistry

http://ejchem.journals.ekb.eg/

Implementation of Nano ZnO Anchored g-C_3N_4 for Biodiesel Production from *Chlorella Sorokiniana* Green Microalgae

Amany Khalifa[a], Maryam Faried[b], Essam M. Abdelsalam[a], Mohamed Samer[b], Mohamed A. Moselhy[c], Yasser A. Attia[a*]

[a] *National Institute of Laser Enhanced Sciences (NILES), Cairo University, Giza 12613, Egypt*

[b] *Department of Agricultural Engineering, Faculty of Agriculture, Cairo University, Giza12613, Egypt*

[c] *Department of Microbiology, Faculty of Agriculture, Cairo University, Giza12613, Egypt*

Abstract

Microalgae show promise for biodiesel production due to their fast growth and high lipid content. However, challenges in cultivation and nutrient supply hinder large-scale production. This study explores the use of ZnO, g-C_3N_4, and ZnO/g-C_3N_4 nanoparticles (NPs) as nutrients to enhance *Chlorella sorokiniana* growth and lipid accumulation. We evaluated the effectiveness of these NPs in cultivating microalgae by supplementing cultures with 15 mg/L of NPs and monitoring key growth parameters. The results indicate that ZnO, g-C_3N_4, and ZnO/g-C_3N_4 NPs positively impact microalgae growth and lipid accumulation. ZnO NPs provide essential zinc micronutrients, while g-C_3N_4 NPs enhance nutrient uptake and enhance the biodiesel production of ZnO NPs from 0.859 times to 1.29 times than the control. The combination of ZnO and g-C_3N_4 NPs exhibits synergistic effects, further improving microalgae growth and lipid content. Lipid analysis shows favorable compositions suitable for biodiesel production. These findings highlight the potential of NPs as nutrient sources for biodiesel production, offering sustainable and cost-effective cultivation methods. This study advances innovative strategies for microalgae-based biodiesel production and underscores the role of nanomaterials in renewable energy.

Keywords: Biodiesel; Microalgae; *Chlorella sorokiniana*; ZnO/g-C_3N_4 Nanocomposite; Biomass Growth; Lipid Accumulation.

1. Introduction

Climate change is a pressing global issue that poses significant challenges to the environment, economies, and societies worldwide. It refers to long-term shifts in temperature patterns and weather conditions, primarily caused by the accumulation of greenhouse gases in the Earth's atmosphere, depleting freshwater resources in some regions, growth in human population, and shortage of agricultural land [1]. Urgent actions are required to mitigate climate change by reducing greenhouse gas emissions and transitioning to renewable energy sources to address this global challenge and safeguard the well-being of current and future generations [2].

Microalgae have emerged as a promising feedstock for biodiesel production due to their high lipid content typically ranging from 20% to 40% of its dry weight, rapid growth rate, and ability to grow in diverse environments [3]. These lipids are composed mainly of triglycerides, which can be converted to biodiesel through transesterification. *Chlorella sorokiniana* has gathered considerable attention for its lipid-rich composition and potential

*Corresponding author e-mail: yasserniles@niles.cu.edu.eg.; (Yasser A. Attia).
EJCHEM use only: Received date 02 November 2023; revised date 18 December 2023; accepted date 27 December 2023
DOI: 10.21608/EJCHEM.2023.246226.8811

as a sustainable biomass source among the various microalgae species [4]. However, the successful cultivation of *Chlorella sorokiniana* on a large scale for biodiesel production requires optimized nutrient availability and cost-effective cultivation strategies. Researchers have explored the utilization of nanomaterials as nutrient sources to enhance microalgae growth rate and biodiesel production [5-7].

Biodiesel has gained significant attention as a renewable and environmentally friendly alternative to conventional fossil fuels, aiming to reduce greenhouse gas emissions and dependence on finite energy resources. Initially, biodiesel was primarily produced from edible oils like sunflower, palm oil, soybean, and other vegetable oils, known as first-generation feedstocks [8]. However, due to the growing world population and decreased reliance on edible oils, there has been a shift towards exploring alternative feedstocks such as salmon oil, sea mango, tobacco seed, jatropha, animal fats, and waste cooking oils [9-11]. These second-generation feedstocks pose challenges for commercial biodiesel production due to their lower energy potential and the need for more efficient technologies.

Microalgae-based biodiesel production holds great promise due to its potential for high lipid productivity, ability to grow in non-arable land and utilize various water sources, and minimal competition with food crops. However, the economic viability of microalgae cultivation for biodiesel production remains a challenge. The cost associated with nutrient supplementation, such as nitrogen, phosphorus, and micronutrients, constitutes a significant portion of the overall production expenses [13]. Therefore, there is a critical need to explore alternative nutrient sources that are cost-effective, sustainable, and capable of enhancing microalgae growth and lipid accumulation [14-16]. The utilization of nanomaterials as nutrient sources in microalgae cultivation offers several advantages over traditional nutrient supplementation. Nanoparticles can provide a controlled and sustained release of nutrients, reducing nutrient loss and improving nutrient utilization efficiency. Additionally, the use of nanomaterials as a nutrient source reduces the reliance on conventional nutrient solutions, which can be costly and may have environmental implications [17]. Furthermore, the application of nanomaterials in biodiesel production from microalgae aligns with the principles of sustainable and green technologies, as it offers the potential for resource efficiency and reduced environmental impact [18-21].

Nanotechnology offers immense potential in various fields, and its application in microalgae cultivation has shown promising results. Nanoparticles possess unique properties, such as high surface area, tunable surface chemistry, and controlled release characteristics, which can significantly impact microalgae growth and lipid production [22,23]. ZnO nanoparticles, g-C_3N_4 NSs, and ZnO/g-C_3N_4 NCs have demonstrated favorable effects on microalgae cultivation, including enhanced cell growth, improved lipid content, and increased lipid productivity [24-26]. Since microalgae have nutritional requirements such as P, N, Ca, K, Mg, Mn, Fe, and Zn, these nutrients have large particle sizes that needs longer time to be absorbed by the cell, which increases the hydraulic retention time of the microalgae [27-29].The release of zinc ions from ZnO nanoparticles contributes to the activation of key enzymes involved in lipid biosynthesis, thereby promoting lipid accumulation in microalgae cells. Similarly, g-C_3N_4 nanoparticles exhibit excellent nutrient adsorption and delivery capabilities, ensuring efficient nutrient uptake by microalgae [30-32]. The incorporation of g-C_3N_4 nanoparticles in microalgae cultivation not only enhances nutrient availability but also a stable growth environment through the prevention of nutrient leaching. By integrating these NPs- based nutrient sources synergetic effects can be achieved leading to further improvements in *Chlorella sorokiniana*biomass productivity and lipid content [33-35].

ZnO nanoparticles offer the advantage of providing essential micronutrients, such as zinc, which are crucial for the growth and development of microalgae. Zinc plays a vital role in various metabolic processes, including lipid synthesis, and its deficiency can limit the productivity of microalgae biomass. On the other hand, g-C_3N_4 nanoparticles possess unique physicochemical properties that can enhance nutrient uptake and utilization in microalgae. The porous structure and

high surface area of g-C_3N_4 nanoparticles facilitate the absorption and transportation of nutrients hence, it can release nitrogen during degradation acting as a nitrogen source for *Chlorella sorokiniana* growth., thereby promoting biomass growth and lipid accumulation. By combining ZnO and g-C_3N_4 nanoparticles in a composite form, synergistic effects may be achieved, further enhancing the growth and lipid content of *Chlorella sorokiniana* [36]. This study aims to explore the effectiveness of ZnO, g-C_3N_4, and ZnO/g-C_3N_4 nanoparticles as nutrient sources for *Chlorella sorokiniana* cultivation and their implications for enhancing biodiesel production.

2. Experimental

The experimental setup involves designing various photobioreactors, selecting appropriate nanomaterials, exposing microalgae to white LEDs, and choosing suitable strains.

2.1. Photobioreactors Design

The photobioreactors were created based on several publications in literature, including [37-39]. These photobioreactors (shown in Figures 1a and 1b) had a 20 cm diameter, 65 cm height, and a 20 L volume. They were constructed locally using Poly (methyl methacrylate), which is also known as acrylic or plexiglass. The photobioreactors have been assembled and are now ready to be used.

2.2. BiostimulationUsing Nanomaterials

For algae to grow, algae require specific nutrients such as nitrogen (N), phosphorus (P), and potassium (K). They also need several other elements like calcium (Ca), magnesium (Mg), manganese (Mn), iron (Fe), boron (B), and zinc (Zn) for healthy growth [40]. To treat the algal cells, some of these nutrients were produced as nanomaterials [41]. The morphology of these nanomaterials, including their size, shape, crystal structure, and optical characteristics, was characterized using transmission electron microscopy (TEM), scanning electron microscopy (SEM), X-ray diffraction (XRD), and steady-state measurements. The preparation processes for the various nanomaterials used in this investigation are described in detail in the following subsections. The additional nanomaterials were photoactivated during the trials, as they were presented to the algae with LEDs.

2.3. g-C_3N_4Nanosheets

The graphitic carbon nitride (g-C_3N_4) powders were synthesized by the direct thermal pyrolysis of urea. 15 g of urea were put in a crucible with a lid, and the process took four hours at a temperature of 550 $^{\circ}$C. More characterization was done on the prepared g-C_3N_4 [27].

2.4. ZnO Nanoparticles

The zinc oxide nanostructure was synthesized by the following method, 15ml of 0.6M of zinc acetate dihydrate and 10ml of 2M of sodium hydroxide were continually stirred for around five minutes each. After thoroughly combining, sodium hydroxide solution was added to the zinc acetate solution while being continuously stirred with a magnetic stirrer for about five minutes. Following that, 100 mL of ethanol was poured into a burette and titrated dropwise to the zinc acetate and sodium hydroxide solution. The process ended in creating a white precipitate. The dry white powder samples were annealed in the air for two hours at 500 °C. [31]

2.5. ZnO/g-C_3N_4Nanocomposites

0.5 g of the prepared g-C_3N_4 NSs were mixed with 0.4 g of the above-prepared ZnO NPs and dissolved in 40 mL of ethanol then stirred for 30 minutes at 80 °C. The obtained solution was centrifuged and washed many times, then the precipitate was dried, and finally, the powder obtained was calcined at 300 °C for 30 minutes. [42].

2.6. Microalgae and Culture Media

2.6.1. Strain of Microalgae

For this study, *Chlorella sorokiniana* SAG 211-8k microalgae were obtained from the Marine Toxin laboratory of the Egyptian Agriculture Research Institute. The strain has low oil content, but it was chosen for experimentation because it is oleaginous. The microalgae were subjected to a red laser as a form of biostimulation, which was hypothesized to increase lipid accumulation [43]. This is particularly important for microalgae with

low oil contents, which typically range between 25% to 35%.

2.6.2. Culture Medium

Blue Green medium (BG11-broth) (Sigma-Aldrich, Germany's) was the sterilized medium that was employed. Sigma-Aldrich created the trace metals for BG-11 by synthesizing them according to established procedures [44].

2.7. Experimental Design

To evaluate the effect of photoactive nanocomposites on the algal biodiesel production 15 L of sterilized BG-11 medium, 15 mg/L each of ZnO NPs, g-C_3N_4 NSs, and ZnO/g-C_3N_4 NCs were dissolved in the medium. For the post-biostimulation process, 5 log10 cell m/L of microalgae inoculums (about 750 mL) were added to 15 L of BG-11 medium and stirred continuously at 30±5°C, CO_2 stream, and at a pH of 7.4. The hydraulic retention time (HRT) of the microalgae inside the reactor was then left for 21 days. These tests were all carried out in duplicate. Centrifugation was used to collect microalgae biomass for 15 minutes at 5000 rpm. The pellets were cleaned, dried at 35 °C, and ground into a fine powder to achieve a constant biomass dry weight. It's important to note that the photobioreactors were exposed to a white LED light source with a wavelength range of 350 –760 nm for a total of 21 days. The light meter (LX-101, Lutron, Taiwan) was used to calculate the light intensity. Klux readings are provided by this gadget (1 Klux = 19.5 µmol/m^2 s). The white LED source used has a 1400 lux light output.

2.8. Calculations

An enhanced Neubauer counting chamber with a surface area of 0.0025 mm^2 and depth of 0.1000 mm was used to count the microalgal cells. 5.15 Log10 cell m/L of microalgae were present at the beginning. The Neubauer counting chamber was used to count cells under the microscope. Cell density was then computed using the formula below [45], and expressed as Log10 cell m/L:

D = *104 (1)

Where A = Total number of counted cells (cell), D = Cell concentration (cell/mL), X = Number of squares.

2.9. Analytical Methods

2.9.1. Oil Extraction

After 21 days of cultivation, the microalgae were collected, and their oil (lipid) was extracted by filtration. Various samples of freeze-dried microalgae were then processed using a Soxhlet Reflux Extractor to extract the total lipids. The extracted lipids were gravimetrically measured in accordance with the published instructions [23,40].

2.9.2. Peroxide Value and Acid Value

Applying the Association of Official Agricultural Chemists (AOAC) method, the peroxide value and the acid value were calculated.

2.10. Transesterification

In a study conducted by Onay et al. [40], oils extracted from biodiesel were characterized and transesterified. This process involved using potassium hydroxide (KOH) and methanol (CH_3OH) to transesterify the oils while agitating for three hours at 60°C. Afterward, the mixture was left to cool to room temperature for 18 hours and a flask separator was used to separate the resulting mixture into biodiesel and glycerol.

2.11. Determination of Fatty Acid Composition

Through the transmethylation of fatty acid chains to fatty acid methyl esters (FAMEs), Zahran and Tawfeuk's (2019) modified approach was used at Cairo University Research Park (CURP), Faculty of Agriculture, to analyze the composition of fatty acids Where gas chromatography (Hewlett Packard, USA) has been performed to separate FAMEs using supelcoTM SP-2380 (60m x 0.25 mm x0.20 µm) column (Sigma- Aldrich, USA) [46]. The report indicates the relative percentage of the total peak after relating the relative and absolute retention times of FAMEs compared to the standards (supelcoTM 37 component FAME mix).

The following equation is used to calculate biodiesel content [47]:

Biodiesel Content (%) = (Σ peak areas of biodiesel FAME compounds / Σ peak areas of all FAME compounds) *100 (2)

To obtain the concentration of biodiesel yield (mg/L) from FAME, the following formula has been used [48,49].

Biodiesel Concentration (mg/L) = (X/100)* V*D*1000 (3)

Whereas:

X: is the percentage of biodiesel.
V: is the volume of biodiesel in the sample.
D: is the density of the biodiesel.

2.12. Transmission electron microscopy imaging

The microalgal cells were separated by centrifugation at 5000 x g for 2 minutes. After that, they were washed three times with phosphate buffer (PB). Glutaraldehyde (2.5%) was used to fix the cells for four hours. The fixed cells were then washed three times for 10 minutes each with PB. Next, osmic acid (1%) was used to fix the cells for 2 hours before washing them again three times with PB for 15 minutes each time. The fixed cells were dehydrated in ethanol with concentrations of 40%, 50%, 60%, 70%, 80%, 90%, 95%, and 100%. After that, propylene oxide was injected into the cells and a resin mixture (Epon 812) was added. Polymerization occurred at 70°C for 9 hours. Tiny pieces (70 nm thick) were cut using an ultramicrotome (RMC Boeckeler, Arizona, USA). Finally, the pieces were mounted onto 200-mesh copper grids and stained with lead citrate for 10 minutes and uranyl acetate (2%). The stained sections were analyzed using a transmission electron microscope (TEM) JEOL-JEM-1200EXII (JEOL Ltd., Tokyo, Japan) operating at 100 kV.

2.13. Statistical Analysis

Statistical analysis has been applied throughout the current investigation to examine the relevance of the various experimental findings. Using the Origin 8 Pro package software, we conducted a one-way ANOVA and Fisher test (P 0.05). (MA, USA).

3. Results and Discussion

3.1. Microalgal Biomass

The fresh weight (FW) and the dry weight (DW) of the used biomass in grams for the different treatments (with nanocomposites addition) and the control (without nanocomposites addition) illustrated in table 1.

The results recommend that the use of different graphitic carbon nitrides with different metal oxide nanomaterials doped in it have a noteworthy influence on the weight of fresh biomass compared to that of the control group and the ZnO NPs group. The utilization of g-C_3N_4 nanocomposites has brought the highest increase in biomass fresh weight (61.2 g). ZnO/g-C_3N_4 NCs have a positive effect on the fresh biomass weights of 47.1g, compared with the control which was only 34.5 g. The improvement effect of these nanomaterials was found to be statistically significant on all levels of comparison except between g-C_3N_4 NSs and ZnO/g-C_3N_4 NCs as both have almost the same effect on the fresh biomass weight. Despite the observation of a slight increase in the dry weight of the biomass after using the prepared nanomaterials, only ZnO/g-C_3N_4 NCs showed a significant increase (10.16 g) when compared to the control experimental group (8.37 g). The other two nanomaterials (ZnO and g-C_3N_4 NSs) induced a statistically insignificant increase in the dry biomass weight (7.1 and 9.07 g, respectively).

Table 1: The composition of *Chlorella sorokiniana* biomass affected by different treatments groups

Treatments	Fresh weight of biomass (g)	Dry weight of biomass (g)	Moisture (%)	Oil content (%)	Biodiesel (g)
Control	34.54±2.88	8.37±0.34	75.70±1.33	7.12±1.48	0.042±0.001
ZnO	35.86±3.73	7.14±0.55	79.98±1.90	10.23±2.56	0.036±0.005
ZnO/ g-C_3N_4	47.12±1.6	10.16±1.26	78.47±1.99	10.04±0.77	0.054±0.011
g-C_3N_4	61.21±6.89	9.01±0.04	85.16±1.58	8.55±0.71	0.058±0.002

3.2. Oil content and moisture

Table 1 illustrates both moisture (%) and oil content (%) for the different treatments (with nanocomposites addition) and the control (without nanocomposites addition). All the utilized nanomaterial mixtures have resulted in increasing the moisture percentage to more than 75.7% for the control group as demonstrated by table 1. All the observed increases between different levels were statistically significant except that between ZnO NPs and g-C_3N_4 NSs since they both led to an increase in the moisture percentage to 80 % and 85.1% respectively. ZnO/g-C_3N_4 NCs give the lowest moisture increase (78.47%). Also, a significant oil production increase was seen in the case of ZnO/g-C_3N_4 NCs (10%), and ZnO NPs (10.23 %) since that of control was only 7.1%. However, because the oil percentage was only 8.55% for g-C_3N_4 NSs, g-C3N4 NSs failed to cause a statistically significant rise in the oil percentage.

3.3. Biodiesel Yield

In the case of producing biodiesel by using different nanomaterial mixtures, table 1 shows that ZnO NPs have a significant decrease in biodiesel

production. g-C_3N_4 NSs resulted in a significant increase (0.058 g/l) when related to biodiesel production by the control group (0.042 g/l). the reduction of biodiesel production that was caused by the usage of ZnO (0.03 mg/L) was found to be statistically significant. Despite, the biodiesel production has increased after the usage of ZnO/g-C_3N_4 NCs (0.054 g/l), it wasn't statistically significant as analyzed by Table 2.

Table 2: Descriptive results of the biodiesel production (mg L^{-1}) by different experimental treated groups

	Sample Size	Mean	Standard Deviation	SE of Mean		
Control	3	0.0420	1E-3	5.773E-4		
ZnO	3	0.0361	0.0051	0.00297		
ZnO/g- C_3N_4	3	0.05433	0.01115	0.00644		
g-C_3N_4	3	0.05833	0.00208	0.0012		
Fisher Test						
	Mean Diff	SEM	t Value	Sig	LCL	UCL
ZnO /Control	-0.00588	0.00415	-1.41734	0	-0.01544	0.00368
ZnO/g-C_3N_4/Control	0.01233	0.0056	2.20332	0	-5.748E-4	0.02524
g-C_3N_4/ Control	0.01633	0.0056	2.91791	1	0.00343	0.02924

3.4. Microalgal Cell Counts

Microalgal cell counts were determined using Neubauer counting chambers. The use of nanomaterials had an impact on *Chlorella* cell numbers. The highest cell counts were observed when zinc oxide/graphitic carbon nitride nanocomposites were used, followed by graphitic carbon nitride nanocomposites, indicating that they enhanced *Chlorella* growth. In contrast to the control, zinc oxide nanoparticles had a minimal inhibitory effect on microalgae proliferation (as shown in Table 3).

Table 3: *Chlorella* cell counts

Treatments	Initial algal load (log10 cell/ml)	Final algal count (log10 cell/ml)	STDEV
Control	5.15	6.99	0.17
ZnO		7.97	0.06
ZnO/g-C_3N_4		7.87	0.33
g-C_3N_4		7.69	0.38

3.5. Fatty Acid Composition

Table 4 demonstrates the metabolomics analysis that was done on over 13 variable crucial fatty acids. Different treatments by different nanomaterials have affected the expression of specific fatty acids. For instance, ZnO/g-C_3N_4 NCs were evident to induce a potent increase in the expression of palmitic and oleic acid in relevance to the control group. Linolic and Eicosapentaenoicfatty acids were seen to be increased as well after the usage of ZnO/g-C_3N_4 NCs. However, ZnO/g-C_3N_4 NCs have led to the reduction of other fatty acid expressions such as lauric, myristic, myristoleic, and other unidentified fatty acids. ZnO NPs have increased the production of Eicosapentaenoicfatty acids when compared to the control, while it caused the reduction of most of the other examined fatty acids when compared to the controls. Finally, g-C_3N_4 NSs have induced the expression of lauric, linoleic, and unidentified fatty acids in relevance to those of the control group. Yet, arachidic, palmitic, eicosapentaenoic, and oleic fatty acids expression was reduced by using g-C_3N_4 NSs as shown in table 4.

3.6. Morphological Changes

According to the results, adding the tested nanoparticles to the *Chlorella* growth media caused alterations in the morphology of the cells. The transmission electron microscope images showed that the size of the cell contents and the number of chloroplasts had increased which can be used as an indication of the changes in the chlorophyll content on the algae cells hence the growth of the microalgae (TEM, Fig.1) in the presence of g-C_3N_4 NSs and ZnO/g-C_3N_4 NCs. Whereas zinc oxide nanoparticles had little inhibitory effect on the microalgal growth as compared to the control [50].

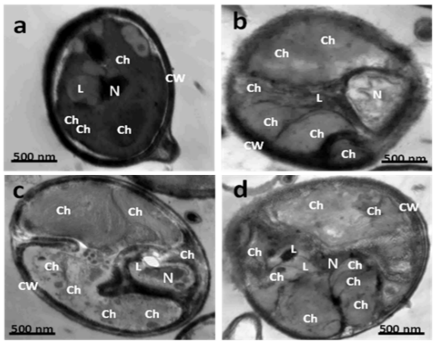

Figure 1: TEM images of cell ultrastructure of *Chlorella sorokiniana* grown in BG11 medium supplemented with nanoparticles: a) control medium, b) zinc oxide NPs, c) graphitic carbon nitride NSs, zinc oxide graphitic carbon nitride NCs. Ch, chloroplast; lipid droplets; N, nucleus; CW, cell wall.

Table 4: The impact of using ZnO, ZnO/g-C_3N_4 and g-C_3N_4 nanomaterials specific fatty acids expression relative to the control group

Fatty acids	Control		ZnO 15 mg/L		(ZnO/g-C_3N_4) 15 mg/L		(g-C_3N_4) 15 mg/L	
	AVE	SD	AVE	SD	AVE	SD	AVE	SD
Caproic acid (C6:0)	–	–	–	–	–	–	0.2025	0.4677
Lauric acid (C12:0)	1.6617	0.2253	0.1700	0.6070	0.2200	0.8663	2.8100	0.2285
Myristic acid (C14:0)	3.9733	0.0208	2.7667	0.4554	1.4200	0.2159	4.5175	0.1172
Myristoleic acid (C14:1)	6.3433	0.2701	3.1067	0.6165	1.1833	0.5677	6.3725	0.3201
Palmitic acid (C16:0)	4.6933	1.8509	5.2667	0.7321	12.2167	2.7998	3.8575	0.9379
Palmitoleic acid (C16:1)	1.1700	0.1114	3.1700	0.2542	4.6467	1.2804	1.0225	0.2676
Stearic acid (C18:0)	2.2683	0.1351	2.2733	0.6067	4.3333	1.1094	1.4675	0.2325
Oleic acid (C18:1)	7.9083	1.0950	8.1867	1.7350	19.5400	4.7444	5.9750	1.0793
Linoleic acid (C18:2)	2.7833	0.7800	2.7667	1.7750	6.0567	4.0079	3.3250	0.6824
Linolenic acid (C18:3)	0.7333	0.7300	1.5733	0.6199	2.6200	0.7355	0.7925	0.9281
Arachidic acid (C20:0)	2.2283	1.4650	0.4433	1.1386	1.2867	0.3522	0.3350	0.7736
Eicosapentaenoic acid (C20:5)	11.2767	9.1900	35.8333	1.3408	20.6900	10.5556	9.2275	0.5458
Lignoceric acid (C24:0)	2.0363	2.0350	–	–	–	–	–	–
Docosahexanoic acid (C22:6)	1.2567	1.2501	–	–	–	–	–	–
Unidentified	51.6670	2.8751	34.4433	4.4660	25.7867	6.6259	60.0950	0.4600

3.7. Characterization of Nanocomposites:

The g-C_3N_4 NSs show a thin wrinkled nanosheet structure (fig. 2a). ZnO nanoparticles were effectively synthesized by the co-precipitation method. The SEM results of ZnO NPs are represented in Figures 2b. A spherical structure with mean diameters of 40 nm is detected for ZnO NPs. The preparing composites of ZnO with g-C_3N_4 resulted in a size decrease to 34nm is shown in figure 2c. The chemical compositions of ZnO NPs and ZnO/g-C_3N_4 NCs were examined using energy dispersive spectroscopy (EDS), which proved the existence of (Zn and O) with (72.58 wt% and 28.42 wt% and (Zn, C, N, and O) with (8.11wt%, 36.89wt%, 37.66wt%, and 17.34wt%), respectively (table 5).

Table 5: EDS results of the prepared nanocomposites, ZnO NPs, ZnO /g-C_3N_4, and g-C_3N_4

Sample	Element	Weight %	Atomic %
ZnO	Zn	72.58	47.74
	O	28.42	52.35
ZnO/g-C_3N_4	C	36.89	6.78
	N	37.66	38.59
	O	17.34	15.55
	Zn	8.11	1.78
g-C_3N_4	C	35.27	39.42
	N	52.47	50.29
	O	12.27	10.29

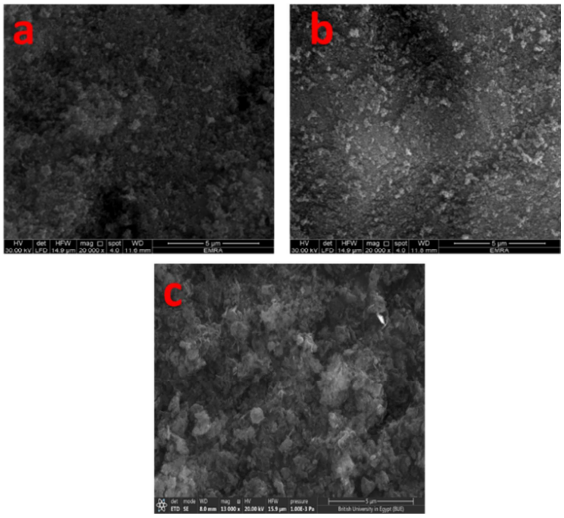

Figure2: SEM images of the prepared g-C_3N_4 NSs (a), ZnO NPs (b), and ZnO/g-C_3N_4 NCs.

The FTIR spectrum (fig. 3) of the g-C_3N_4 NSs peak at 810 cm^{-1} belongs to the stretching mode of the triazine units in g-C_3N_4 NSs, in which peaks at 1145, 1213, 1393, 1587, and 1648 cm^{-1} were assigned to the stretching vibrations of aromatic rings' skeletal stretching modes in CN heterocycles. The distinctive bands in the FTIR spectra of ZnO/g-C_3N_4 NCs include the C-N stretching vibration mode at wavenumber 1634 cm^{-1} and the aromatic C-N stretching modes at wavenumbers 1318, 1411, and

1643 cm^{-1}. The out-of-plane bending modes of C-N heterocycles are responsible for the band seen at 801 cm^{-1}. The stretching vibration of ZnO was attributed to the peak at 566 cm^{-1}. A large absorption peak at 3384 cm^{-1} was also caused by the presence of water molecules. The FTIR spectrum of ZnO NPs, which widths the wavelength range of 390 to 4000 cm^{-1}, is shown in fig. 3. A large vibration band with a wavelength between 400 and 500 cm^{-1} is attributed to the Zn-O bond's distinctive stretching mode. Stretching is indicated by hydroxyl groups from absorbed H_2O molecules in the wide peak 3434 cm^{-1}.

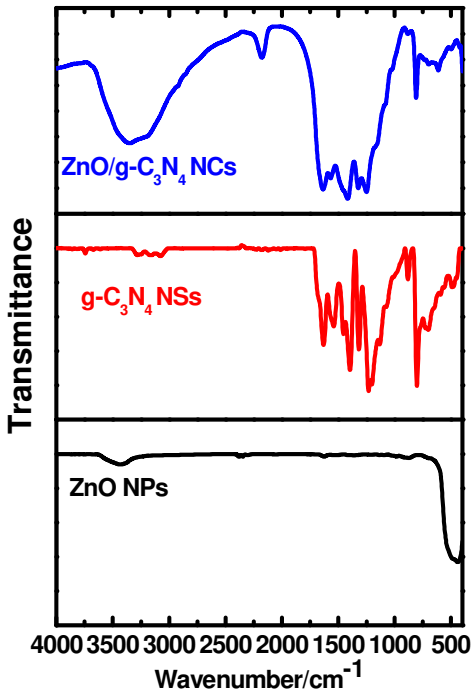

Figure 3: the FTIR analysis of the prepared nanomaterials; ZnO NPs, g-C_3N_4 NSs, and ZnO/g-C_3N_4 NCs.

The planes (100), (002), (101), (102), and (110) are represented by the angles of 31.79°, 34.42°, 36.25°, 47.44°, and 56.53° in the XRD pattern of ZnO NPs, respectively (fig. 4). The (100) and (002) planes, respectively, correspond to the two main diffraction peaks for pure g-C_3N_4 at 13.1° and 27.5°. The weaker peak at the (100) plane in graphitic materials results from the stacking of aromatic rings between interlayers, whereas the stronger peak at the (002) plane is caused by the interlayer distance on the g-C3N4 NSs. Nevertheless, specific diffraction peaks for g-C_3N_4 NSs were not observed in the 1D ZnO/g-C_3N_4 films.

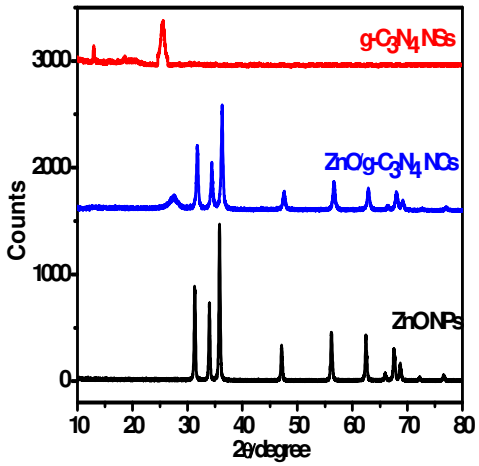

Figure 4: XRD analysis of the prepared nanomaterials; ZnO NPs, g-C_3N_4 NSs, and ZnO/g-C_3N_4 NCs

Algae reproduce quickly and can collect many high-energy lipids because of their photosynthetic activities, making algae one of the most abundant sources of renewable fuels [12]. Algae also have a multitude of benefits, such as a simple life cycle and easy access to resources for mass production [12]. In addition to producing oxygen and fixing CO_2 from the environment, algae have a high oil production that can be recovered by destroying their cell structure [23]. Algae's main benefit is its capacity to transform the biomass it produces into a range of biofuels [51]. Light, which is simple to control, is the primary component that stimulates microalgae to accumulate oil. As a result, laser radiation can be used to increase lipid content via light [52]. The most promising alternative to normal diesel is biodiesel. Because biodiesel has combustion qualities that are remarkably comparable to those of petroleum diesel, it can be used in engines work by diesel without requiring engine changes to help satisfy the world's energy needs [51]. According to the findings of this investigation, the addition of either 15 mg/l of g-C_3N_4 NSs or photoactivated ZnO/g-C_3N_4 NCs produced the maximum biodiesel yield (0.058 g/l) due to algae, like any other living organisms, require certain essential nutrients to support their growth and metabolic processes. One of the key nutrients necessary for algae growth is nitrogen (N). Nitrogen is an essential component of proteins, amino acids, nucleic acids, and chlorophyll—the pigment responsible for photosynthesis. Nitrogen availability plays a crucial role in regulating algal growth and biomass production. In environments where nitrogen is limited, such as in some freshwater systems or

during certain seasons, algae growth can be restricted. Conversely, excessive nitrogen levels, often resulting from pollution or eutrophication, can lead to algal blooms and ecological imbalances. The uptake and utilization of nitrogen by algae involve various metabolic pathways and enzymatic processes. Algae can adapt to different nitrogen sources and exhibit varying preferences for specific forms of nitrogen depending on their species and environmental conditions. To optimize algae cultivation for various applications, including biofuel production, it is important to understand and manage the nitrogen requirements of specific algal species. By providing adequate nitrogen sources in appropriate forms and concentrations, the growth and productivity of algae can be enhanced while minimizing environmental impacts. In this work, N is presented in the form of g-C_3N_4 nanosheets. In contrast to prior investigations, discovered that 0.06 g of biodiesel was created per kilogram of microalgae after being exposed to a red laser made of Helium-Neon (He-Ne) [49]. In contrast, Khalifa et al. (2022) found that adding ferric oxide (Fe_2O_3) at 1.2 mg/L, manganese dioxide (MnO_2) at 1 mg/L, magnesium oxide (MgO) at 7.3 mg/L, and zinc oxide (ZnO) at 5 mg/L each produced different amounts of microalgae: 0.0445, 0.0354, 0.0307, and 0.0289 g biodiesel /L, respectively [33]. According to a different study by Faried et al. (2022), adding calcium chloride ($CaCl_2$) at a concentration of 2 mg /L, potassium chloride (KCl) at a concentration of 4.5 mg /L, and ferric chloride ($FeCl_3$) at a concentration of 1.2 mg /L produced 0.0307, 0.0353, and 0.0444 g of biodiesel /L microalgae, respectively. A further study by Faried et al. (2023) found that the addition of ammonium carbonate $(NH_4)_2CO_3$ with a concentration of 72 mg/L, monocalcium phosphate $Ca(H_2PO_4)_2$ with a concentration of 14 mg/L, potassium carbonate (K_2CO_3) with a concentration of 4.5 mg/L, and calcium carbonate ($CaCO_3$) with a concentration of 2 mg/L delivered 0.0753, 0.062, 0.0326, and 0.0382 g biodiesel per liter microalgae, respectively [53]. Beginning with the Hydraulic Retention Time (HRT) and continuing throughout the entire testing period, photoactivated nanomaterials had biostimulating effects on the algae. Additionally, the time required to obtain the highest yield of oil and biodiesel, which is the production's peak, as well as the lag phase, was shortened by the addition of nanomaterials. This generally agrees with past studies on various bacteria used to produce biofuels [40, 54]. Therefore, the prepared nanoparticles have shown potential for enhancing biodiesel production from algae through various mechanisms. Here are a few impacts of nanoparticles on biodiesel production from algae:

Nutrient Delivery and Uptake Enhancement: Nanoparticles can serve as carriers for nutrient delivery to the algae culture, improving nutrient availability and uptake. For example, studies have demonstrated the use of nanoparticles like zinc oxide (ZnO) and graphene-based nanomaterials (such as graphene oxide and reduced graphene oxide) to enhance nutrient supply and uptake in algae cultures [55-57].

Growth Promotion: Certain nanoparticles have been found to promote algal growth by providing essential nutrients or acting as growth stimulants. For instance, iron oxide nanoparticles (Fe_3O_4 NPs) have been shown to enhance algal growth and lipid accumulation in species like *Chlorella* vulgaris and Scenedesmus obliquus [58,59].

Lipid Accumulation Enhancement: Nanoparticles can also contribute to increased lipid accumulation in algae, which is a crucial factor for biodiesel production. Studies have reported the use of nanoparticles like magnetic nanoparticles, g-C_3N_4, and SiC nanoparticles to enhance lipid productivity in different algal species [60, 61].

Enzyme and Catalyst Immobilization: Nanoparticles can serve as supports for immobilizing enzymes or catalysts involved in the transesterification process, which is a key step in biodiesel production. This immobilization improves enzymatic activity and enhances the efficiency of the transesterification reaction, leading to improved biodiesel yields [62].

4. Conclusions

According to the findings of this study, supplementing the microalgae with 15 mg/l of photoactivated ZnO/g-C_3N_4 NCs or 15 mg/l of g-C_3N_4 NSs yields the most biodiesel. When compared to any other experimental treatment group, the control treatment, i.e., without the addition of photoactivated nanomaterials, yields the least amount of biodiesel. As a result, this study suggests incorporating nanotechnology into the algal biodiesel production process by adding nanomaterials (nutrients) to microalgae culture broth, which is an effective technique for green microalgae treatment that can be combined with modern algal biodiesel production units.

5. Conflicts of interest

There are no conflicts to declare.

6. Formatting of funding sources

The authors would like to acknowledge the Science and Technology Development Fund (STDF) of Egypt for funding this paper through research projects number 26272.

7. Acknowledgments

The authors would like to acknowledge the Science and Technology Development Fund (STDF)

of Egypt for funding this paper through research projects number 26272.

7. References

[1]. Schaller N., Kay A.L., Lamb R., Massey N. R., Oldenborgh G. J., Otto F. E. L., Sparrow S. N., Vautard R., Yiou P., Ashpole I., Bowery A., Crooks S. M., Haustein K., Huntingford C., Ingram W. J., Jones R. G., Legg T., Miller J., Skeggs J., Wallom D., Weisheimer1 A., Wilson S., Stott P. A., Allen M. R., Human influence on climate. Southern England winter foods and their impacts, Nature climate change 2016, (6), 627-634.

[2]. Hughes T.P., Kerry J.T., Álvarez-Noriega M., Álvarez-Romero J.G., Anderson K.D., Baird A. H, Babcock R. C., Beger M., Bellwood D.R., Berkelmans R. M., Bridge T. C., Butler I. R., Byrne M., Cantin N.E., Comeau S., Connolly S.R., Cumming G.S., Dalton S.J., Diaz-Pulido G., Eakin C. M., Figueira W. F., Gilmour J.P., Harrison H.B., Heron S.F., Hoey A.S., Hobbs J.-P.A., Hoogenboom M.O., Kennedy E.V., Kuo C., Lough J.M., Lowe R.J., Liu G., McCulloch M.T., Malcolm H.A., McWilliam M.J., Pandolfi J. M., Pears R. J., Pratchett M.S., Schoepf V., Simpson T., Skirving W.J., Sommer B., Torda G., Wachenfeld D.R., Willis B.L., Wilson S.K., Global warming and recurrent mass bleaching of corals, Nature. 2017, (543). 373-377.

[3]. Dolganyuk V., Belova D., Babich O., Prosekov A., Ivanova S., Katserov D., Patyukov N., Sukhikh S., Microalgae: A Promising Source of Valuable Bioproducts, Biomolecules. 2020 10(8), 1153. doi: 10.3390/biom10081153.

[4]. Powers S. E., Baliga R., Sustainable algae biodiesel production in cold climates, Int. J. Chem. Eng., 2010, 102179.doi: 10.1155/2010/102179.

[5]. Veillette M., Chamoumi M., Nikiema J., Faucheux N., Heitz M., Production of Biodiesel from Microalgae, Advances in Chemical Engineering, 2012, 245. doi: 10.5772/31368.

[6]. Akso F., Koru Y. E., Alparslan M., Microalgae for Renewable Energy: Biodiesel Production and other Practices, Journal of Science and Technology, 2014, 2, 167–174.

[7]. Ghorbani A., Rahimpour M.R., Ghasemi Y., Raeissi S., The Biodiesel of Microalgae as a Solution for Diesel Demand in Iran, Energies, 2018, 11(4), 950. https://doi.org/10.3390/en11040950

[8]. Babajide O., Sustaining Biodiesel Production via Value-Added Applications of Glycerol, J. Energy, 2013, 2023, 178356. doi: 10.1155/2013/178356.

[9]. Behera S., Singh R., Arora R., Sharma N.K., Shukla M., Kumar S., Scope of algae as third generation biofuels, Front BioengBiotechnol. 2015, 2, 90. doi: 10.3389/fbioe.2014.00090.

[10]. Bezergianni S., Dimitriadis A., Comparison between different types of renewable diesel, Renew. Sustain. Energy Rev., 2012, (21), 110–116, doi: 10.1016/j.rser.2012.12.042.

[11]. Ma Y., Wang Z., Yu C., Yin Y., Zhou G., Evaluation of the potential of 9 Nannochloropsis strains for biodiesel production, Bioresour Technol. 2014, 167, 503-9. doi: 10.1016/j.biortech.2014.06.047.

[12]. Kim GV, Choi W, Kang D, Lee S, Lee H. Enhancement of biodiesel production from marine alga, Scenedesmus sp. through in situ transesterification process associated with acidic catalyst, Biomed Res Int. 2014, 2014, 391542. doi: 10.1155/2014/391542.

[13]. Lau Z.L., Low S.S., Ezeigwe E.R., Chew K.W., Chai W.S., Bhatnagar A., Yap Y.J., Show PL. A review on the diverse interactions between microalgae and nanomaterials: Growth variation, photosynthetic performance and toxicity, Bioresour Technol. 2022, 351, 127048. doi: 10.1016/j.biortech.2022.127048.

[14]. Attia Y. A., Kobeasy M. I., Samer M., Evaluation of magnetic nanoparticles influence on hyaluronic acid production from *Streptococcus equi*, Carbohydr. Polym., 2018, 192, 135-142. doi: 10.1016/j.carbpol.2018.03.037.

[15]. Zhu L. D., Li Z. H., Hiltunen E., Strategies for Lipid Production Improvement in Microalgae as a Biodiesel Feedstock, Biomed Res. Int., 2016, 2016, 8792548. doi: 10.1155/2016/8792548.

[16]. Zhong L., Feng Y., Wang G., Wang Z., Bilal M., Lv H., Jia S., Cui J., Production and use of immobilized lipases in/on nanomaterials: A review from the waste to biodiesel production, Int. J. Biol. Macromol., 2020, (152), 207–222, doi: 10.1016/j.ijbiomac.2020.02.258.

[17]. Nguyen M. K., Moon J., Khac V., Bui H., Oh Y., Lee Y., Recent advanced applications of nanomaterials in microalgae biorefinery, Algal Res., 2019, 41, 101522. doi: 10.1016/j.algal.2019.101522.

[18]. Yadala S. Cremaschi S., Design and optimization of artificial cultivation units for algae production Design and optimization of arti fi cial cultivation units for algae production, Energy, 2018, 78(C), 23-39. doi: 10.1016/j.energy.2014.06.001.

[19]. Abdelsalam E., Samer M., Abdel-hadi M. A., Hassan H. E., Badr Y., In fluence of laser irradiation on rumen fluid for biogas production from dairy manure, Energy, 2018, 163, 404–415. doi: 10.1016/j.energy.2018.08.118.

[20]. Alos R., Types of microorganisms, Global Journal of Microbiology Research, 2022, 10(1), 403. doi: 10.15651/GJMR.22.10.403.

[21]. Álvarez-díaz P. D., Ruiz J., Arbib Z., Barragán J., Garrido-pérez M. C., Perales J. A., Freshwater microalgae selection for simultaneous wastewater nutrient removal and lipid production, Algal Research, 2017, 24, 477–485. doi: 10.1016/j.algal.2017.02.006.

[22]. Zhao Y., Gui L., Chen Z., Sensors and Actuators B: Chemical Colorimetric detection of Hg 2+ based on target-mediated growth of gold nanoparticles, Sensors Actuators B. Chem., 2017, 241, 262–267. doi: 10.1016/j.snb.2016.10.084.

[23]. Hijazi O., Abdelsalam E., Samer M., Amer B.M.A., Yacoub I.H., Moselhy M.A., Attia Y.A., Bernhardt H., Environmental impacts concerning the addition of trace metals in the process of biogas production from anaerobic digestion of

slurry, J. Clean. Prod., 2020, 243, 118593. doi: 10.1016/j.jclepro.2019.118593.
[24]. Reddy K. R., Reddy C. V., Nadagouda M. N., Shetti N. P., Jaesool S., Aminabhavi T. M., Polymeric graphitic carbon nitride (g-C3N4)-based semiconducting nanostructured materials: Synthesis methods, properties and photocatalytic applications, J. Environ. Manage., 2019, 238, 25–40. doi: 10.1016/j.jenvman.2019.02.075.
[25]. Ejikeme P. M., Anyaogu I. D., Ejikeme C. L., Nwafor N. P., Egbuonu C. A. C., Ukogu K., Ibemesi J. A., Catalysis in Biodiesel Production by Tranesterification Process-An Insight, Journal of Chemistry, 2010, 7(4), 1120-1132.
[26]. Xie B., Tang X., Yong H., Deng S., Shi X., Biological sulfamethoxazole degradation along with anaerobically digested centrate treatment by immobilized microalgal-bacterial consortium: Performance, mechanism and shifts in bacterial and microalgal communities, Chem. Eng. J., 2020, 388, 124217. doi: 10.1016/j.cej.2020.124217.
[27]. Zhang K., Kurano N., Miyachi S., Optimized aeration by carbon dioxide gas for microalgal production and mass transfer characterization in a vertical flat-plate photobioreactor, Bioprocess and Biosystems Engineering, 2002, 25, 97–101. doi: 10.1007/s00449-002-0284-y.
[28]. Wigger H., Steinfeldt M., Banchin A., Environmental benefits of coatings based on nano-tungsten-carbide cobalt ceramics, J. Clean. Prod., 2017, 148, 212-222 doi: 10.1016/j.jclepro.2017.01.179.
[29]. Rezania S., Oryani B., Park J., Hashemi B., Yadav K. K., Kwon E. E., Hur J., Cho J., Review on transesterification of non-edible sources for biodiesel production with a focus on economic aspects, fuel properties and by-product applications, Energy Convers. Manag., 2019, 201, 112155. doi: 10.1016/j.enconman.2019.112155.
[30]. Grima E. M., Camacho F. G., Pérez J. A. S., Sevilla J. M. F., Fernández F. G. A., Gómez A. C., A mathematical model of microalgal growth in light-limited chemostat culture, Journal of Chemical Technology and Biotechnology, 1994, 61(2), 167-173.
[31]. Kumar S. S., Venkateswarlu P., Rao V. R., Rao G. N., Synthesis, characterization and optical properties of zinc oxide nanoparticles, 2013, 3, 30. doi: 10.1186/2228-5326-3-30.
[32]. Chandran A. Prakash J., Naik K. K., Srivastava A. K., Dąbrowski R., Czerwińskic M., Biradar A. M., Preparation and characterization of MgO nanoparticles/ferroelectric liquid crystal composites for faster display devices with improved contrast, J. Mater. Chem. C, 2014, 2, 1844-1853 doi: 10.1039/c3tc32017k.
[33]. Khalifa A., Faried M., Abdelsalam E., Attia Y. A., Moselhy M. A., Yousef R. S., Samer M., Effects of Fe2O3, MnO2, MgO and ZnO additives on lipid and biodiesel production from microalgae, Egyptian Journal of Chemistry, 2022, 65(1), 511–519. doi: 10.21608/EJCHEM.2021.82155.4051.
[34]. Attia Y. A., Abdelsalam E. M., Saeed S., Saleh M. M., Samer M., Bioethanol Production from Potato Peels Using *Saccharomyces cerevisiae* Treated with ZnO and ZnO/g-C3N4 Nanomaterials, Egyptian Journal of Chemistry, 2022, 65(131), 309–315. doi: 10.21608/EJCHEM.2022.118978.5351.
[35]. Khan M., Farah H., Iqbal N., Noor T., Bin Amjad M. Z., Bukhari S. S. E., A TiO2 composite with graphitic carbon nitride as a photocatalyst for biodiesel production from, RSC Adv., 2021, 11, 37575–37583. doi: 10.1039/D1RA07796A.
[36]. Dey N., Vickram S., Thanigaivel S., Manikandan S., Subbaiya R., Karmegam N., Kim W., Govarthanan M., Aftermath of nanomaterials on lipid profile of microalgae as a radical fuel supplement – A review, Fuel, 2023, 333(P2), 126444. doi: 10.1016/j.fuel.2022.126444.
[37]. Luo H.P., Al-Dahhan M.H., Analyzing and modeling of photobioreactors by combining first principles of physiology and hydrodynamics. BiotechnolBioeng. 2004, 85(4), 382-93. doi: 10.1002/bit.10831.
[38]. Ugwu C. U., Aoyagi H., Uchiyama H., Photobioreactors for mass cultivation of algae, Bioresource Technology, 2008, 99(10), 4021–4028. doi: 10.1016/j.biortech.2007.01.046.
[39]. Petcharoen K., Sirivat A., Synthesis and characterization of magnetite nanoparticles via the chemical co-precipitation method, Mater. Sci. Eng. B, 2012, 177(5), 421–427. doi: 10.1016/j.mseb.2012.01.003.
[40]. Lam M. K., Lee K. T., Khoo C. G., Uemura Y., Lim J. W., Growth kinetic study of *Chlorella vulgris* using lab-scale and pilot-scale photobioreacter: effect of CO_2 concentration, Journal of Engineering Science and Technology Special Issue on SOMCHE 2015, 2016, 73–87.
[41]. Vasistha S., Khanra A., Rai M. P., Influence of microalgae-ZnO nanoparticle association on sewage wastewater towards efficient nutrient removal and improved biodiesel application: An integrated approach, J. Water Process Eng., 2021, 39, 101711. doi: 10.1016/j.jwpe.2020.101711.
[42]. Manimozhi R., Mathankumar M., Prakash A. P. G., Synthesis of g-C_3N_4/ZnO heterostructure photocatalyst for enhanced visible degradation of organic dye, Optik, 2021, 165548. doi: 10.1016/j.ijleo.2020.165548.
[43]. Faried M., Samer M., Moselhy M. A., Yousef R. S., Ali A. S., Ahmed R. H., Marrez D. A., El-Hussein A., Abdelsalam E. M., Photobiostimulation of green microalgae *Chlorella sorokiniana* using He-Ne red laser radiation for increasing biodiesel production. Biomass Conversion and Biorefinery, 2022. DOI:https://doi.org/10.1007/s13399-021-02220-3
[44]. Stanier R. Y., Kunisawa R., Mandel M., Purification and Properties of Unicellular Blue-Green Algae (Order Chroococcales), 1971, 35(2), 171–205.
[45]. Trinh D. M., Nguyen T. T., Nguyen P. K., Tran N. Q. A., Vo C. T., The effect of nutrients on the growth of microalgae *Haematococcuslacustris* (Girod-chantrans) Rostafinski 1875. Int.J.Curr.Res.Biosci.Plantbio l2019, 6(4), 17-23.

[46]. Zahran H. A., Tawfeuk H. Z.,Physicochemical properties of new peanut (Arachis hypogaea L.) varieties. OCL, 2019, 26, 19. https://doi.org/10.1051/ocl/2019018
[47]. Zhang S., Zhang L., Xu G., Li F., Li X, A review on biodiesel production from microalgae: Influencing parameters and recent advanced technologies. Front. Microbiol. 2022, 13, 970028. doi: 10.3389/fmicb.2022.970028
[48]. Simbi I., Osagie U., Oyekanmi O., Adelaja O., Energy Conversion and Management: X Chemical and quality performance of biodiesel and petrol blends, Energy Convers. Manag. 2022, 15, 100256. doi: 10.1016/j.ecmx.2022.100256.
[49]. Waickman Z., Loyola University of Chicago: Biodiesel Labs. 2017. 5. 1–72.
[50]. Faried M., Khalifa A., Samer M., Attia Y. A., Moselhy M. A., El-Hussein A., Yousef R. S., Abdelbary K., Abdelsalam E. M., Biostimulation of green microalgae *Chlorella sorokiniana* using nanoparticles of MgO, $Ca_{10}(PO_4)6(OH)_2$, and ZnO for increasing biodiesel production. Scientific Reports 2023, 13, 19730.
[51]. Gholami A., Pourfayaz F., Maleki A., Recent Advances of Biodiesel Production Using Ionic Liquids Supported on Nanoporous Materials as Catalysts: A Review, Front. Energy Res., 2020, 8, 144. doi: 10.3389/fenrg.2020.00144.
[52]. Abdelsalam E. M., Samer M., Attia Y. A., Abdel-Hadi M. A., Hassan H. E., Badr Y., Effects of Laser Irradiation and Ni Nanoparticles on Biogas Production from Anaerobic Digestion of Slurry, Waste and Biomass Valorization, 2019, 10(11), 3251–3262, 2019, doi: 10.1007/s12649-018-0374-y.
[53]. Faried M., Khalifa A., Abdelsalam E., Attia Y., Moselhy M. A., Yousef R. S., Abdelbary K., Samer M., Impacts of $(NH_4)_2CO_3$, $Ca(H_2PO_4)$, K_2CO_3 and $CaCO_3$ additives on biodiesel production from algae. Egypt J Chem 2023, 66(8), 47-57.
[54]. Scheufele F. B., Hinterholz C. L., Zaharieva M. M., Najdenski H. M., Módenes A. N., Trigueros D. E. G., Borba C. E., Espinoza-Quiñones F. R., Kroumov A. D., Complex mathematical analysis of photobioreactor system, 2019, 19(12), 844–859. doi: 10.1002/elsc.201800044.
[55]. Paucar N.E., Sato C., Microbial Fuel Cell for Energy Production, Nutrient Removal and Recovery from Wastewater: A Review. *Processes*. 2021; 9(8):1318. https://doi.org/10.3390/pr9081318
[56]. Attia Y. A.,Samer M.,Mohamed M. S. M., Moustafa E., Salah M., Abdelsalam E. M., Nanocoating of microbial fuel cell electrodes for enhancing bioelectricity generation from wastewater, Biomass Conversion and Biorefinery, 2022. https://doi.org/ 10.1007/s13399-022-02321-7
[57]. Yuan X., Gao X., Liu C., Liang W., Xue H., Li Z., Jin H., Application of Nanomaterials in the Production of Biomolecules in Microalgae: A Review. Marine Drugs. 2023, 21(11), 594. https://doi.org/10.3390/md21110594
[58]. Rana M. S., Bhushan S., Sudhakar D. R., Prajapati S. K., Effect of iron oxide nanoparticles on growth and biofuel potential of *Chlorella spp.,* Algal Research, 2020, 49, 101942.
[59]. Bibi M., Zhu X., Munir M., Angelidaki I., Bioavailability and effect of α-Fe_2 O_3 nanoparticles on growth, fatty acid composition and morphological indices of *Chlorella vulgaris*. Chemosphere, 2021, 282, 131044. https://doi.org/10.1016/j.chemosphere.2021.131044
[60]. Parandi E., Safaripour M., Abdellattif M. H., Saidi M., Bozorgian A., Nodeh H. R., Rezania S., Biodiesel production from waste cooking oil using a novel biocatalyst of lipase enzyme immobilized magnetic nanocomposite, Fuel, 2022, 313, 123057.
[61]. Ren H.-Y., Dai Y.-Q., Kong F., Xing D., Zhao L., Ren N.-Q., Ma J., Liu B.-F., Enhanced microalgal growth and lipid accumulation by addition of different nanoparticles under xenon lamp illumination, Bioresource Technology, 2020, 297, 122409.
[62]. Qian J., Huang A., Zhu H., Ding J., Zhang W., Chen Y., Immobilization of lipase on silica nanoparticles by adsorption followed by glutaraldehyde cross-linking. Bioprocess Biosyst Eng. 2023, 46(1), 25-38. doi: 10.1007/s00449-022-02810-z.